Inorg. Chem. **2007**, *46*, 1259−1267

Sulfur K-edge Spectroscopic Investigation of Second Coordination Sphere Effects in Oxomolybdenum-Thiolates: Relationship to Molybdenum−Cysteine Covalency and Electron Transfer in Sulfite Oxidase

Katrina Pearisо,[†] Matthew E. Helton,[†] Eileen N. Duesler,[†] Susan E. Shadle,[‡] and Martin L. Kirk*,[†]

Department of Chemistry, The University of New Mexico, MSC03 2060, 1 University of New Mexico, Albuquerque, New Mexico 87131-0001, and Department of Chemistry, MS 1520, Boise State University, 1910 University Drive, Boise, Idaho 83725

Received June 23, 2006

Second-coordination sphere effects such as hydrogen bonding and steric constraints that provide for specific geometric configurations play a critical role in tuning the electronic structure of metalloenzyme active sites and thus have a significant effect on their catalytic efficiency. Crystallographic characterization of vertebrate and plant sulfite oxidase (SO) suggests that an average O_{oxo}–Mo–S_{Cys}–C dihedral angle of ∼77° exists at the active site of these enzymes. This angle is slightly more acute (∼72°) in the bacterial sulfite dehydrogenase (SDH) from *Starkeya novella*. Here we report the synthesis, crystallographic, and electronic structural characterization of Tp*MoO(mba) (where Tp* = (3,5-dimethyltrispyrazol-1-yl)borate; mba = 2-mercaptobenzyl alcohol), the first oxomolybdenum monothiolate to possess an O_{ax}–Mo–$S_{thiolate}$–C dihedral angle of ∼90°. Sulfur X-ray absorption spectroscopy clearly shows that O_{ax}–Mo–$S_{thiolate}$–C dihedral angles near 90° effectively eliminate covalency contributions to the Mo(*xy*) redox orbital from the thiolate sulfur. Sulfur K-pre-edge X-ray absorption spectroscopy intensity ratios for the spin-allowed S(1s) → S^{v}(p) + Mo(*xy*) and S(1s) → S^{v}(p) + Mo(*xz*,*yz*) transitions have been calibrated by a direct comparison of theory with experiment to yield thiolate S^{v}(p) orbital contributions, c_i^2, to the Mo(*xy*) redox orbital and the Mo(*xz*,*yz*) orbital set. Furthermore, these intensity ratios are related to a second coordination sphere structural parameter, the O_{oxo}–Mo–$S_{thiolate}$–C dihedral angle. The relationship between Mo–$S_{thiolate}$ and Mo–$S_{dithiolene}$ covalency in oxomolydenum systems is discussed, particularly with respect to electron-transfer regeneration in SO.

Introduction

Sulfite oxidizing enzymes are ubiquitous in nature, having been found in animal, plant, and bacterial species.[1] Vertebrate and plant sulfite oxidases (SO) and the sulfite dehydrogenase (SDH) from *Starkeya novella* catalyze the oxidation of sulfite to sulfate, the terminal step in the degradation of sulfur-containing amino acids, in addition to various other sulfur-containing chemicals non-native to the organism, such as sulfa drugs. The oxidized resting-state active site of SO and SDH, $[(dt)MoO_2(S_{Cys})]^-$ (where dt = dithiolene), consists of a five-coordinate Mo(VI) ion possessing both apical and equatorial oxo donors, two sulfur donors from the dithiolene chelate,[2] and a single cysteine thiolate (S_{Cys}) donor that provides the only covalent linkage between the cofactor and the protein (Scheme 1).[3,4] The substrate sulfite is oxidized to sulfate during catalysis, with the Mo(VI) center being reduced to Mo(IV). It has been suggested that the attack of the sulfite lone pair on the equatorial oxo ligand (O_{eq}) results in the population of a Mo−O_{eq} d_{xy}−p_{π} antibonding orbital, which has been hypothesized to labilize the equatorial oxygen atom for transfer to the substrate.[5] In vertebrate SO, two subsequent one-electron transfers to the endogenous b_5-type

* To whom correspondence should be addressed. Phone: (505) 277-5992. E-mail: mkirk@unm.edu. Fax: (505) 277-2609.
[†] University of New Mexico.
[‡] Boise State University.

(1) Hille, R. *Chem. Rev.* **1996**, *96*, 2757−2816.
(2) Kirk, M. L.; Helton, M. E.; McNaughton, R. L. *Prog. Inorg. Chem.* **2004**, *52*, 111−212.
(3) George, G. N.; Garrett, R. M.; Prince, R. C.; Rajagopalan, K. V. *J. Am. Chem. Soc.* **1996**, *118*, 8588−8592.
(4) Kisker, C.; Schindelin, H.; Pacheco, A.; Wehbi, W.; Garrett, R.; Rajagopalan, K.; Enemark, J.; Rees, D. *Cell* **1997**, *91*, 973−983.

10.1021/ic061150z CCC: $37.00
Published on Web 02/12/2007

Scheme 1. Generalized Catalytic Cycle for SO, Including Structures for Catalytically Relevant Species. SO_{ox} Is Oxidized SO, SO_{red} Represents Reduced SO Forms, *hpH* and *lpH* Are High pH and Low pH Epr Active Mo(V) Enzyme Forms, Respectively

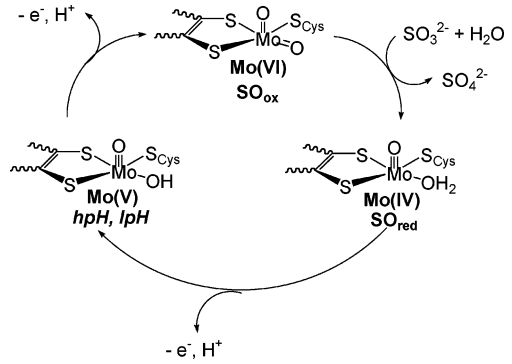

heme, and ultimately to *cyt*C, return the Mo active site to the dioxomolybdenum $[(dt)Mo^{VI}O_2(S_{Cys})]^-$ resting state.[6,7]

The development of model systems is necessary in order to understand how individual aspects of the first and second coordination spheres affect the ground state electronic structure of the active site, redox potentials, electron-transfer regeneration, and oxo-transfer catalysis. Two major synthetic challenges have impeded the progress of model systems for SO. The first is that it is difficult to synthesize a five-coordinate mononuclear molybdenum site while also preventing Mo dimer formation. The second challenge reflects the difficulty in generating a low-symmetry model with two different types of sulfur donors, dithiolene and thiolate, that can provide the necessary insight into the electronic structure of the SO active site. These challenges were elegantly overcome by Lim et al.,[8] who reported the synthesis of $(Et_4N)[MoO_2(SC_6H_2\text{-}2,4,6\text{-}^iPr_3)(bdt)]$ (bdt = benzene-1,2-dithiolate), an exact first coordination sphere model of the dioxomolybdenum(VI) form of SO with an $O_{oxo}-Mo-S_{thiolate}-C$ dihedral angle of ~46°. Interestingly, this model did not display an electronic absorption spectrum similar to that observed for *Arabidopsis thaliana* SO, which lacks the *b*-type heme that obscures the spectrum of the Mo domain in chicken SO.[8,9] Specifically, the electronic absorption spectrum of $(Et_4N)[MoO_2(SC_6H_2\text{-}2,4,6\text{-}^iPr_3)(bdt)]$ completely lacks the 496 nm band, assigned as a $S_{Cys}\rightarrow Mo$ charge-transfer transition, in the enzyme spectrum.[9] Therefore, we have hypothesized that second coordination sphere effects at the active site may, in part, explain the observed differences in both the charge-transfer spectra and ground state electronic structures of the enzyme and small molecule analogue.[5,10,11]

The effect of the $O_{oxo}-Mo-S_{thiolate}-C$ dihedral angle on Mo−S covalency has not been quantified, although this second coordination sphere structural parameter on $S\rightarrow Mo$ charge transfer intensity and redox potentials in oxomolybdenum thiolate complexes has been previously explored.[5,10,11] Detailed spectroscopic and DFT studies, conducted by McNaughton et al.,[12−14] examined the effect of changing the $O_{oxo}-Mo-S_{thiolate}-C$ dihedral angle on the overlap between the Mo(*xy*) redox orbital and a thiolate p orbital (S^v). The thiolate S^v orbital is oriented orthogonal to the Mo−S bond and is primarily involved in π-bonding interactions with the metal. The results suggest that both the amount of S^v orbital character covalently mixed into the Mo(*xy*) singly occupied molecular orbital (SOMO), or redox orbital, and the LMCT intensity should follow a $\cos^2 x$ function of the $O_{oxo}-Mo-S_{thiolate}-C$ dihedral angle (x).[12−14] This theoretical work anticipated that when the dihedral angle is near 90°, $S^v-Mo(xy)$ covalency and the intensity of the $S^v\rightarrow Mo(xy)$ charge-transfer bands decrease to zero. However, this angular dependence has not been examined experimentally. Interestingly, the $O_{oxo}-Mo-S_{Cys}-C$ dihedral angles obtained from the crystal structures of chicken liver SO (~80°),[15] *A. thaliana* SO (~74°),[16] and *S. novella* SDH (~72°)[17] are all relatively close to 90°, suggesting that there is very little overlap between the coordinated cysteine thiolate S^v_{Cys} orbitals and the Mo(*xy*) redox orbital in both oxidized and reduced forms of the enzyme.[5] Thus, the observed $O_{oxo}-Mo-S_{Cys}-C$ dihedral angle in the enzymes is not expected to confer appreciable $S^v-Mo(xy)$ covalency, which should result in a $S_{Cys}\rightarrow Mo(xy)$ charge-transfer transition in either oxidized, (SO_{ox}), or reduced paramagnetic (SO_{red}) forms of SO that possesses very low charge transfer intensity.[5,10,11,18,19]

Recently, we reported the synthesis and spectral characterization of models for the paramagnetic Mo(V) electron-transfer intermediate in SO.[10,11] Spectroscopic studies of paramagnetic forms of the enzyme, as well as their small-molecule analogues, are important, as these systems are related to the obligatory Mo(V) intermediate in the electron transfer (oxidative) half-reaction of SO. These new model systems employ the (2-dimethylethanethiol)bis(3,5-dimethylpyrazolyl)methane (L3SH) heteroscorpionate ligand which provides an equatorial thiolate donor with a relatively constrained $O_{oxo}-Mo-S_{L3S}-C$ dihedral angle.[10] This molecule was specifically designed to probe the synergistic interactions between thiolate and dithiolene donors and their combined effect on the electronic structure of the oxomolybdenum(V) site. The $O_{oxo}-Mo-S_{L3S}-C$ dihedral angle in [(L3S)MoO(bdt)] was determined to be 115° by X-ray crystallography,[10] and this is slightly closer (by ~6°) to 90°

(5) Pearisо, K.; McNaughton, R. L.; Kirk, M. L. *J. Am. Chem. Soc.* **2002**, *124*, 9006−9007.
(6) Brody, M. S.; Hille, R. *Biochemistry* **1999**, *38*, 6668−6677.
(7) Pacheco, A.; Hazzard, J. T.; Tollin, G.; Enemark, J. H. *J. Biol. Inorg. Chem.* **1999**, *4*, 390−401.
(8) Lim, B. S.; Willer, M. W.; Miao, M. M.; Holm, R. H. *J. Am. Chem. Soc.* **2001**, *123*, 8343−8349.
(9) Garrett, R. M.; Rajagopalan, K. V. *J. Biol. Chem.* **1996**, *271*, 7387−7391.
(10) Pearisо, K.; Chohan, B.; Carrano, C.; Kirk, M. *Inorg. Chem.* **2003**, *42*, 6194−6203.
(11) Kirk, M. L.; Pearisо, K. *Polyhedron* **2004**, *23*, 499.
(12) McNaughton, R. L.; Tipton, A. A.; Rubie, N. D.; Conry, R. R.; Kirk, M. L. *Inorg. Chem.* **2000**, *39*, 5697−5706.
(13) McNaughton, R. L.; Helton, M. E.; Cosper, M. M.; Enemark, J. H.; Kirk, M. L. *Inorg. Chem.* **2004**, *43*, 1625−1637.
(14) McNaughton, R. L.; Mondal, M. S.; Nemykin, V. N.; Basu, P.; Kirk, M. L. *Inorg. Chem.* **2005**, *44*, 8216−8222.
(15) Kisker, C.; Schindelin, H.; Pacheco, A.; Wehbi, W. A.; Garrett, R. M.; Rajagopalan, K. V.; Enemark, J. H.; Rees, D. C. *Cell* **1997**, *91*, 973−983.
(16) Schrader, N.; Fischer, K.; Theis, K.; Mendel, R. R.; Schwarz, G.; Kisker, C. *Structure* **2003**, *11*, 1251.
(17) Kappler, U.; Bailey, S. *J. Biol. Chem.* **2005**, *280*, 24999.
(18) Kirk, M.; Pearisо, K. *Curr. Opin. Chem. Biol.* **2003**, *7*, 220−227.
(19) Kirk, M. L.; Pearisо, K. *J. Inorg. Biochem.* **2003**, *96*, 61.

than the corresponding dihedral angle in model compounds that employ thiolate donors that are not part of a chelate ring.[8] Interestingly, the lowest field component (g_1) of the anisotropic *g*-tensor for [(L3S)MoO(bdt)] was observed to be $g_1 = 2.016$, which is larger than that measured for either the low pH (*lpH*) ($g_1 = 2.007$) or high pH (*hpH*) ($g_1 = 1.999$) forms of SO.[10,20] These observations were interpreted in the context of a significantly greater degree of $S^v(p)-Mo(xy)$ covalency in [(L3S)MoO(bdt)] than in the *lpH* or *hpH* forms of the chicken enzyme, and this likely results from the greater deviation of the $O_{ax}-Mo-S_{thiolate}-C$ dihedral angle from 90° in the model than in the enzymes. This interpretation is also consistent with the observation that $g_1 > g_e$ for the model, which is only anticipated in the presence of appreciable $S^v(p)-Mo(xy)$ covalency and charge-transfer contributions to *g*-tensor anisotropy.[10,21,22]

Our prior work suggested that the $O_{oxo}-Mo-S_{thiolate}-C$ dihedral angle controls $Mo-S_{thiolate}$ covalency contributions to the Mo(*xy*) orbital. In this study, we use XAS at the S K-edge to understand and quantitate the influence of this dihedral angle on $S^v(p)-Mo(xy)$ and $S^v(p)-Mo(xz,yz)$ covalency in oxomolybdenum thiolates, including a newly structurally characterized complex, Tp*MoO(mba) (where Tp* = (3,5-dimethyltrispyrazol-1-yl)borate; mba = 2-mercaptobenzyl alcohol) which possesses a 95° $O_{oxo}-Mo-S_{thiolate}-C$ dihedral angle. The $O_{ax}-Mo-S_{thiolate}-C$ dihedral angle is shown to have a pronounced effect on the relative intensity ratios of the XAS spin-allowed $S(1s)\rightarrow S^v(p) + Mo(xy)$ and $S(1s)\rightarrow S^v(p) + Mo(xz,yz)$ transitions. Here, we use a combination of experiment and theory to determine thiolate $S^v(p)$ orbital contributions, c_i^2, to the Mo(*xy*) redox orbital and to relate these intensity ratios to the $O_{oxo}-Mo-S_{thiolate}-C$ dihedral angle. The relationship between this dihedral angle and $Mo-S_{thiolate}$ covalency, as well as its influence on electron-transfer regeneration in SO and SDH, is also discussed.

Experimental

Preparation of Compounds. The synthesis of Tp*MoO(mba) followed the synthetic scheme developed by Cleland et.al.[23] A dry toluene solution containing 0.287 g (2.08 mmol) of H_2mba and 290 μL (2.08 mmol) of triethylamine was added dropwise by cannula at 70 °C to a dry toluene solution of Tp^*MoOCl_2 (0.499 g, 1.04 mmol). The solution was allowed to react for ~13 h, during which time the color of the solution changed from lime green to dark green. The resulting dark green solution was filtered and concentrated under vacuum to precipitate a dark green powder. The powder was redissolved in a minimum amount of toluene and chromatographed on silica gel using a 1.5 in. (diameter) × 8 in. (length) column and a binary mixture of toluene/1,2-dichloroethane (4:1) as the eluent. The third eluate was a large dark green band that yielded 0.427 g of Tp*MoO(mba) as a dark green powder (75%). Crystals suitable for X-ray crystallography and analytical data were obtained by recrystallization from methanol. Anal. Calcd for $C_{22}H_{28}N_6O_2SBMo$ (547.32 g/mol): C, 48.28; H, 5.16; N, 15.36. Found: C, 47.58; H, 5.62; N, 14.84. IR (KBr, cm^{-1}): $\nu(Mo^V{\equiv}O)$ 937, ν(B−H) 2540. MS (FAB): $m/z = 549$ (parent ion), 454 (parent − 3,5 dimethylpyrazole), 411 (parent − 2-mercaptobenzylate ligand). Elemental analysis was performed at Galbraith Laboratories in Knoxville, TN, and the FAB mass spectrum was collected at The Nebraska Center for Mass Spectrometry in the Department of Chemistry at the University of Nebraska−Lincoln.

The complexes $PPh_4[MoO(SPh)_4]$ (SPh = benzenethiol), Tp*MoO(bdt), and Tp*MoO(SPh)Cl were prepared as previously described[23] and characterized by electronic absorption and EPR spectroscopies prior to their use in the S XAS experiments.

Physical Methods. General. Solution electronic absorption spectra were collected using a Hitachi-3501 UV−vis−NIR dual-beam spectrophotometer. The electronic absorption spectra were measured in 1 cm path length, black-masked, Wilmad quartz cuvettes. Solution and frozen glass EPR spectra were measured at X-band (~9.3 GHz) using a Bruker EMX spectrometer. The room-temperature solution spectra were measured in dichloromethane. For the low-temperature measurements, a 1:1 toluene/dichloromethane mixture was used as a glassing solvent, and the temperature was held at 25 K in an Oxford liquid helium flow cryostat.

S XANES Measurements. S K-edge XANES were measured at the National Synchrotron Light Source under dedicated conditions (2.9 GeV, 150 mA) on beamline X19A using a Rh-coated focusing mirror and a Si(111) double-crystal monochromator detuned 50% for harmonic rejection. The X19A end station includes a He flight path to minimize attenuation of the low-energy X-ray beam. All of the measurements were made at room temperature as fluorescence excitation spectra using a PIPS detector (Canberra). The samples were prepared by grinding solid samples into a fine powder and spreading them into a thin layer on polyethylene tape (Esco, Tuscon). The samples were placed in a flowing He sample chamber for the duration of the measurements. Two to three scans were measured for each sample over the 2322−2722 eV energy range using a step size of 0.1 eV over the S K-edge (2462−2492 eV) and Mo L3- (2512−2542 eV) and L2-edges (2612−2642 eV). The energy was calibrated by measuring the spectrum of a sublimed elemental S calibration foil between each sample and assigning the inflection point of this spectrum to 2472 eV.

XANES data were normalized by fitting the data below and above the S K-edge to the McMaster X-ray absorption cross-sections. Due to the presence of the Mo L3-edge, the post-edge region was limited to the region of 2480−2520 eV for all of the complexes, and therefore, care was taken to use the same background subtraction parameters for all of the data sets to facilitate comparison. The features in the pre-edge region were quantitated by spectral fitting using the program EDG_FIT. EDG_FIT was written by Dr. Graham N. George of the University of Saskatchewan and distributed with the EXAFSPAK suite of programs (http://ssrl.slac.stanford.edu/EXAFSPAK.html).[24] This program uses the double-precision version of the public domain MINPAK fitting library. The pre-edge features and the rising edge functions were fit using pseudo-Voigt line shapes. The ratio of Gaussian/Lorentzian contribution, the energy, and the intensity of each feature was allowed to vary in the fitting procedure. Since there were only two pre-edge features in these complexes, this produced eight variable parameters in each fit, which was well

(20) Bray, R. C.; Gutteridge, S.; Lamy, M. T.; Wilkinson, T. *Biochem. J.* **1983**, *211*, 227−236.
(21) Balagopalakrishna, C.; Kimbrough, J. T.; Westmoreland, T. D. *Inorg. Chem.* **1996**, *35*, 7758−7768.
(22) Swann, J.; Westmoreland, T. D. *Inorg. Chem.* **1997**, *36*, 5348−5357.
(23) Cleland, W. E.; Barnhart, K. M.; Yamanouchi, K.; Collison, D.; Mabbs, F. E.; Ortega, R. B.; Enemark, J. H. *Inorg. Chem.* **1987**, *26*, 1017−1025.
(24) Pickering, I.; George, G. *Inorg. Chem.* **1995**, *34*, 3142−3152.

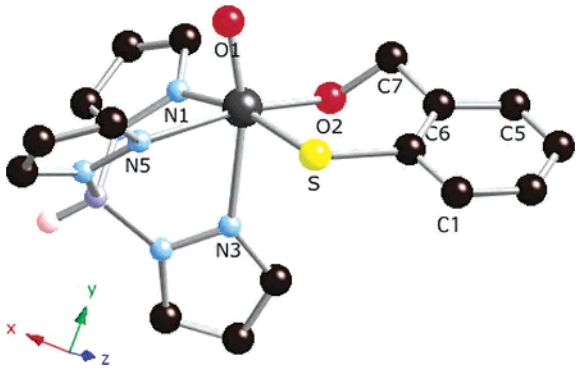

Figure 1. Molecular structure of Tp*MoO(mba). Methyl groups and hydrogens of the ligands have been removed for clarity. Relevant bond lengths and bond angles are given in Table 1.

Table 1. Selected Bond Distances and Bond Angles for Tp*MoO(mba)

bond distances		bond angles	
Mo-N1	2.187(3)	O1−Mo−S−C1	−95.49(17)
Mo-N5	2.205(3)	O1−Mo−S	102.05(11)
Mo-N3	2.341(3)	O2−Mo−S	87.84(8)
Mo-O1	1.676(2)	O1−Mo−N3	164.27(13)
Mo-O2	1.903(2)	N1−Mo−N5	86.72(12)
Mo−S	2.397(1)		

within the number of independent data points over the fitting range of 2465−2474 eV. The area of each peak was determined by numerical integration. Because there is a certain amount of error associated with direct quantitative comparison of normalized absorption features from different spectra, in order to make semiquantitative comparisons between the pre-edge features of the S XANES spectra, the intensity of the individual pre-edge features were normalized to the total fitted area of the pre-edge. This treatment removes the intensity variation due to the spectral normalization from the quantitative comparison of the individual pre-edge features.

X-ray Crystallography. The crystal structure of Tp*MoO(mba) was obtained at The University of New Mexico X-ray Laboratory located in the Department of Chemistry. Suitable crystals were grown by slow evaporation of methanol and mounted in glass capillaries. The crystals were then centered on a Bruker P4 automated diffractometer, and determinations of space group, orientation matrix, and unit cell dimensions were performed in a standard manner. Crystallographic data were collected in the ω scan mode using a Mo Kα radiation source ($\lambda = 0.71073$ Å), a highly oriented graphite crystal monochromator, a scintillation counter, a pulse height analyzer, and XSCANS software (Siemens, 1994). The solution and refinement of the structures were performed with the SHELXL97 program.[25] The systematic absences in the diffraction pattern are consistent with a *P*21/*c* space group for Tp*MoO(mba). All of the hydrogen atoms were treated as idealized contributions using a riding model. Complete structural parameters are provided in the Supporting Information.

Results and Analysis

Molecular Structure of Tp*MoO(mba). The X-ray crystal structure of Tp*MoO(mba) is presented in Figure 1, and selected bond distances and angles are tabulated in Table 1. The data reveal a distorted six-coordinate geometry about the Mo(V) ion, similar to that of other structurally characterized Tp*MoOL$_2$ species. Typical Mo−N bond distances are observed, with the expected elongation of the Mo−N3 bond oriented trans to the strong-field apical oxo donor (Table 1). The cis orientation of the apical oxo and the thiolate donor ligands in Tp*MoO(mba) results in an O1−Mo−S bond angle of 102.05(11)°, which is very similar to the O_{ax}−Mo−S_{Cys} angle determined from X-ray crystallographic studies of the chicken liver enzyme.[15] However, the most important structural feature in Tp*MoO(mba) relative to the enzymes is the ∼95° O1−Mo−S−C1 dihedral angle. This angle in Tp*MoO(mba) is markedly different than that observed in $[MoO(SPh)_4]^{1-}$ (∼59°) .[12−14] The key point here, vide infra, is that the O_{ax}−Mo−S−C dihedral angles of Tp*MoO(mba) and enzymes are close to 90°. As such, Tp*MoO(mba) represents an ideal structural model for providing new and detailed insight into important Mo(*xy*)−S_{cys}(p) orbital interactions, including the role of the cysteine thiolate in reduced forms of SO. This is of particular importance with respect to how the coordinated cysteine ligand may affect the reduction potential of the reduced site and contribute to electron-transfer regeneration in sulfite oxidizing enzymes.

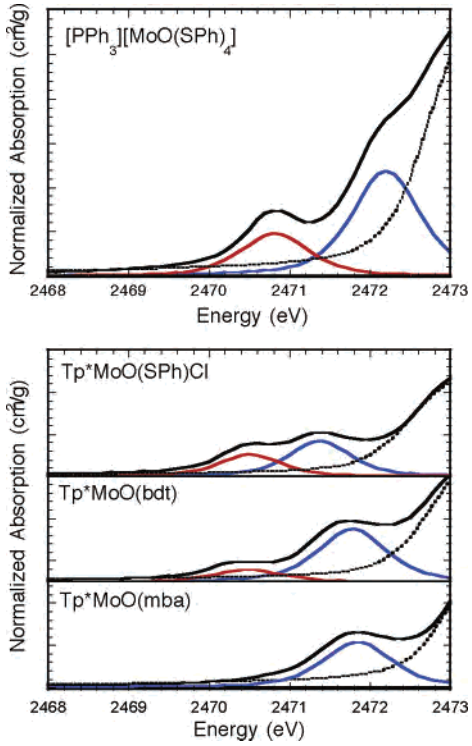

Figure 2. Top: Normalized S K-edge XAS of $[PPh_3][MoO(SPh)_4]$. Bottom: Normalized S K-edge XAS for Tp*MoO(SPh)Cl, Tp*MoO(bdt), and Tp*MoO(mba). The pseudo-Voigt resolved S(1s)→S^v(3p) + Mo(*xy*) transition is in red, the S(1s)→S^v(3p) + Mo(*xz*,*yz*) transition is in blue, and the contribution from the rising edge is in black (dashed). Peak energies, relative peak areas, and percent thiolate character mixed in to Mo(*xy*) and Mo(*xz*,*yz*) are given in Table 3.

Ligand K-Edge X-ray Absorption Spectroscopy. Figure 2 displays the S XANES pre-edge region of the high-symmetry (∼C_4) oxomolybdenum tetrathiolate complex, $PPh_4[MoO(SPh)_4]$, the oxo-molybdenum monothiolate complexes Tp*MoO(mba) and Tp*MoO(SPh)Cl, and the oxo-molybdenum *dithiolene*, Tp*MoO(bdt). The S K-edge spectra of $PPh_4[MoO(SPh)_4]$, Tp*MoO(SPh)Cl, and Tp*MoO(bdt)

(25) Sheldrick, G. M. *SHELXTL*, 5.10; Bruker Analytical X-ray: Madison, WI, 1997.

each possess two distinct pre-edge features. The S K-edge energy separations of these two peaks are similar to the S^{v}-(3p)→Mo(*xy*) and S^{v}(3p)→Mo(*xz*,*yz*) charge-transfer transition energy differences determined from detailed analyses of the S→Mo charge-transfer spectra for a number of oxomolybdenum(V) models.[12−14,26,27]

X-ray absorption spectroscopy at the S K-edge is among the most powerful and direct spectroscopic probes of thiolate ligand covalency in the overall metal−ligand bonding scheme.[28] This results from the fact that transitions in the near-edge region are bound state transitions and arise from dipole allowed S(1s) core one-electron promotions to valence orbitals that possess S(3p) character. There are three energetically inequivalent thiolate S(3p) orbitals in oxomolybdenum thiolates that are potentially involved in the Mo−$S_{thiolate}$ bonding scheme. The situation is somewhat different in oxomolybdenum mono-dithiolenes.[2] Although a dithiolene possesses three S(3p) orbitals per sulfur donor, there are *two* sulfur donors in a dithiolene and a unique electronic structure relative to single thiolate donors.[2] Thus, O_{oxo}−Mo−$S_{thiolate}$−C dihedral angles approaching 90° in oxomolybdenum *thiolates* result in negligible Mo(d_{xy})−S(p) orbital overlap. In contrast, appreciable Mo(d_{xy})−S(p) orbital overlap is present in oxomolybdenum *dithiolenes* when the O_{oxo}−Mo−$S_{dithiolene}$−C dihedral is ∼90°.[2] Relevant metal−ligand orbital interactions for oxomolybdenum thiolates and dithiolenes are depicted in Figure 3. Since all three S(3p) orbitals are completely occupied, the S K-edge transitions are formally described as S(1s)→S(3p) + Mo(4d) (Figure 4), with intensities that are directly proportional to the square of the S(3p) atomic orbital coefficient (c_i) in the LCAO expansion of the formally Mo(4d) orbitals (Ψ_i^*) according to

$$\Psi^* = \sqrt{1 - c_i^2}\,\mathrm{Mo(4d)} - c_i\mathrm{S(3p)} \qquad (1)$$

The S^{π}/C^{σ}(3p) orbital in oxomolybdenum thiolates is at deepest binding energy and dominantly involved in intraligand S−C σ-bonding. Because this orbital is unavailable for bonding with the Mo d orbitals, one will not observe pre-edge transitions to MOs involving this S 3p orbital. However, the S^{π}/C^{σ}(3p)* orbital, which possesses S−C σ* character, does contribute at higher energies to the S K-edge spectrum in the form of the intense "white line" feature at or near the edge position. The S^{σ}(3p) orbital is primarily σ-bonding with the Mo(x^2-y^2) orbital and the degree of its covalency is relatively unaffected by the orientation of the O_{oxo}−Mo−$S_{thiolate}$−C dihedral angle. In contrast, the nature of the Mo−S^{v}(3p) bonding interaction is highly dependent on the O_{oxo}−Mo−$S_{thiolate}$−C dihedral. As such, a single S^{v}(3p) orbital may interact with Mo(*xy*), a component of the pseudo-degenerate Mo(*xz*,*yz*) orbital set, or both. The S^{ip}(a″) orbital in oxomolybdenum dithiolenes is σ bonding

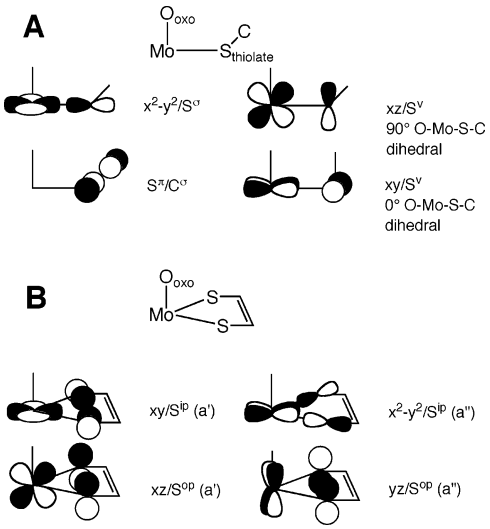

Figure 3. Idealized Mo−S bonding interactions in oxomolybdenum thiolates (A) and dithiolenes (B). The coordinate system is such that the Mo(*xy*) orbital bisects the M−L bonds. The S^{σ} orbital is bonding with Mo(x^2-y^2) in the oxomolybdenum thiolates, the S^{π}/C^{σ} orbital is nonbonding with the metal due to a large energy stabilization resulting from S−C bonding, and the S^{v} orbital is bonding with Mo(*xy*) and/or Mo(*xz*,*yz*) depending on the nature of the O_{oxo}−Mo−$S_{thiolate}$−C dihedral angle. In dithiolene systems, the S^{ip} orbital of a′ symmetry is pseudo-σ bonding with Mo(*xy*), the S^{op} orbitals are bonding with the Mo(*xz*,*yz*) orbital set, and the S^{ip} orbital of a″ symmetry is σ bonding with Mo(x^2-y^2). In marked contrast to the oxomolydenum thiolate bonding scheme, the dithiolenes possess significant Mo−S covalency when the O_{oxo}−Mo−$S_{dithiolene}$−C dihedral angle is ∼90°.

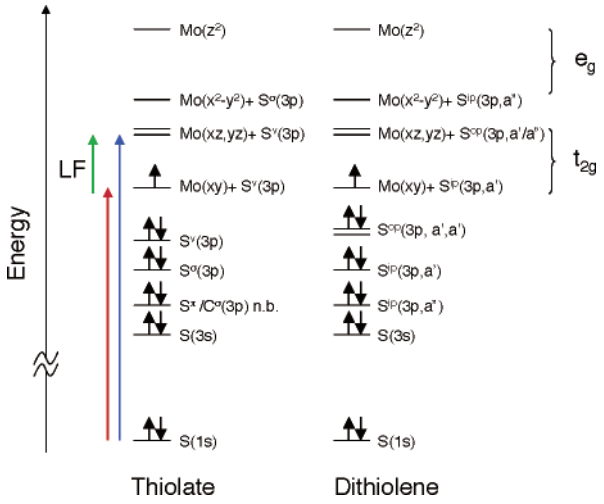

Figure 4. Depiction of the key S(1s)→S^{v}(3p) + Mo(*xy*) and S(1s)→S^{v}(3p) + Mo(*xz*,*yz*) pre-edge transitions in the S K-edge experiment. The t_{2g} and e_g labels refer to the orbital labels in an O_h ligand field. Ideally, with no electronic relaxation, the energy of the ligand field (LF) transition should be equal to the energy difference between the two XAS pre-edge transitions.

with Mo(x^2-y^2), lies deepest in binding energy, and does not appreciably mix with the other $S_{dithiolene}$ valence orbitals.[2] The S^{ip}(a′) orbital primarily forms a pseudo-σ bonding interaction with Mo(*xy*), and the S^{op}(a′,a″) orbitals are bonding with respect to Mo(*xz*,*yz*). Mixing between the S^{ip}(a′) and S^{op}(a′) orbitals has been shown to occur in low-symmetry environments.[2] Thus, the lower-energy S K-pre-edge transition is appropriately assigned as S(1s)→S^{v}(3p) + Mo(*xy*) in oxomolybdenum thiolates and S(1s)→S^{ip}(3p,a′) + Mo(*xy*) in the dithiolenes, while the higher-energy transition is

(26) Inscore, F.; McNaughton, R.; Westcott, B.; Helton, M.; Jones, R.; Dhawan, I.; Enemark, J.; Kirk, M. *Inorg. Chem.* **1999**, *38*, 1401−1410.
(27) McMaster, J.; Carducci, M. D.; Yang, Y. S.; Solomon, E. I.; Enemark, J. H. *Inorg. Chem.* **2001**, *40*, 687.
(28) Solomon, E. I.; Randall, D. W.; Glaser, T. *Coord. Chem. Rev.* **2000**, *200*, 595−632.

Table 2. List of O≡Mo−S−C Dihedral Angles for the Oxomolybdenum Thiolates and the Dithiolene Tp*MoO(bdt) Used in this Study

compound	O≡Mo−S−C dihedral angle	ref
$[MoO(SPh)_4]^{1-}$	59° (av)	12,13
Tp*MoO(mba)	95.5°	this work
Tp*MoO(SPh)Cl	n.a.	n.a.
Tp*MoO(bdt)	81.5° (av)	23

assigned as S(1s)→S^v(3p) + Mo(*xz*,*yz*) in the thiolates and S(1s)→S^{op}(3p,a′/a″) + Mo(*xz*,*yz*) in oxomolybdenum dithiolenes (Figure 4).

At this point, we will focus on the relative intensity differences of these two pre-edge transitions in oxomolybdenum thiolates and develop relationships between the O_{oxo}−Mo−$S_{thiolate}$−C dihedral angle and Mo−$S_{thiolate}$ covalency. Since the S K-pre-edge oscillator strengths (integrated intensities) are proportional to the S^v(p) character, c_i^2, covalently mixed into Mo(*xy*) and Mo(*xz*,*yz*), we can quantitatively determine the S^v(p) covalency contributions to the Mo−$S_{thiolate}$ bonding scheme.[29] It should be noted that the transition probability for a spin-allowed S(1s)→S^v(p) + Mo(*xy*) transition is half the transition probability for the S(1s)→S^v(p) + Mo(*xz*,*yz*) transition. This results from the fact that there is only a single hole in the d^1 Mo(*xy*) redox orbital while two holes are present in a single component of the degenerate Mo(*xz*,*yz*) orbital set. As such, the intensity of the S(1s)→S^v(p) + Mo(*xz*,*yz*) transition, $I_{xz,yz}$, must be scaled by a factor of 0.5 in order to make direct comparisons between the relative S^v(p) content (c_i) covalently mixed into Mo(*xy*) and the Mo(*xz*,*yz*) component.

In order to make quantitative covalency comparisons between oxomolybdenum thiolates, the S K-pre-edge intensities must be calibrated against covalency parameters determined by independent methods. Detailed DFT and spectroscopic studies have been performed on the high-symmetry ($\sim C_4$) oxo-molybdenum thiolate complex, $PPh_4[MoO(SPh)_4]$.[12−14,27] The data show that 6.6% and 10.8% S^v(3p) orbital character per thiolate is covalently mixed into Mo(*xy*) and the Mo(*xz*,*yz*) orbital set, respectively, when the O_{oxo}−Mo−$S_{thiolate}$−C dihedral angle is ∼59°. This allows for the application of group overlap integrals, defined as <S^v(3p)|Mo(*xy*)> and <S^v(3p)|Mo(*xz*,*yz*)>, to determine the degree of S^v(3p) character covalently mixed into Mo(*xy*) and Mo(*xz*,*yz*) as a function of the O_{oxo}−Mo−$S_{thiolate}$−C dihedral angle (Table 2). We have proposed that the O_{oxo}−Mo−$S_{thiolate}$−C dihedral angle affects the degree of S^v(3p)−Mo(*xy*) and S^v(3p)−Mo(*xz*,*yz*) orbital mixing and that the square of the c_i's scale with the square of the projection ($\cos^2 x$) of the S^v(3p) orbital on to Mo(*xy*) and Mo(*xz*,*yz*).[13] A plot of $\cos^2 x$ as a function of the O_{oxo}−Mo−$S_{thiolate}$−C dihedral angle in $PPh_4[MoO(SPh)_4]$ is shown in Figure 5. The maximum in $\cos^2 x$ has been scaled to ∼25.0% S^v(3p) using the calculated 6.6% S^v(3p) orbital character mixed into the Mo(*xy*) orbital when the O_{oxo}−Mo−$S_{thiolate}$−C dihedral angle is ∼59° (i.e., 6.6%/$\cos^2$ (59°) = 25%). Thus, maximum S^v(3p)−Mo(*xy*) orbital overlap is achieved when the O_{oxo}−Mo−$S_{thiolate}$−C dihedral angle is 0° or 180° (i.e., a π bond with Mo(*xy*)).

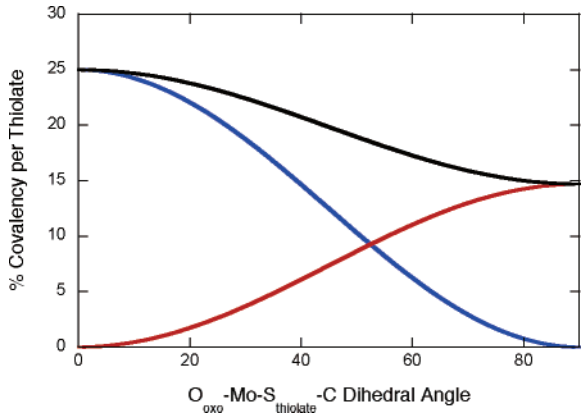

Figure 5. Molybdenum−sulfur covalency as a function of the O_{oxo}−Mo−$S_{thiolate}$−C dihedral angle. Blue line: %S character in Mo(*xy*); red line: %S character in Mo(*xz*,*yz*); black line: total S character in the t_{2g}-derived orbital set.

Interestingly, the 0°/180° O_{oxo}−Mo−$S_{thiolate}$−C dihedral represents the minimum in <S^v(3p)|Mo(*xz*,*yz*)> overlap, and we assign this a value of 0.0% S^v(3p) covalently mixed into Mo(*xz*,*yz*). Maximum S^v(3p)−Mo(*xz*,*yz*) overlap occurs when the O_{oxo}−Mo−$S_{thiolate}$−C dihedral angle is 90°, and the maximum S covalency mixed in to Mo(*xz*,*yz*) has been scaled to ∼14.7% S^v(3p) using the calculated 10.8% S^v(3p) orbital character per thiolate mixed into the Mo(*xz*,*yz*) orbital set of $PPh_4[MoO(SPh)_4]$ when the O_{oxo}−Mo−$S_{thiolate}$−C dihedral angle is ∼59° (i.e., 10.8%/$\cos^2$ (90° − 59°) = 14.7%). Inspection of the S K-pre-edge data for $[MoO(SPh)_4]^{1-}$ in Figure 2 allows for the DFT-derived covalency parameters to be evaluated experimentally. The integrated intensity ratio, $I_{xz,yz}/2I_{xy}$, determined for $[MoO(SPh)_4]^{1-}$ is 1.3, which is in quite good agreement with the ratio of the DFT-calculated S^v(3p) orbital character (i.e., 10.8%/6.6% = 1.6) mixed into Mo(*xy*) and Mo(*xz*,*yz*) at a O_{oxo}−Mo−$S_{thiolate}$−C dihedral angle of ∼59°. In order to test this idea further, we refer to a related study on *cis*,*trans*-(L-N_2S_2)MoO(X) (where L-N_2S_2 = *N*,*N*′-dimethyl-*N*,*N*′-bis(2-mercaptophenyl)-ethylenediamine and X = $SCH_2C_6H_5$, $SC_6H_4OCH_3$, or $SC_6H_4CF_3$) which detailed the covalency contributions to oxomolybdenum thiolate bonding with one of the O_{oxo}−Mo−$S_{thiolate}$−C dihedral angles being ∼180°.[13] Here it was found that ∼22% S^v(3p) orbital character is covalently mixed into Mo(*xy*), which compares very nicely to the 25% predicted from our model, vide supra. As such, measurement of the S K-pre-edge ratio, $I_{xz,zy}/2I_{xy}$, for oxomolybdenum thiolates allows for the experimental determination of key Mo(4d)−S(3p) covalency parameters.

The S K-pre-edge intensity ratio, $I_{xz,zy}/2I_{xy}$, in oxomolybdenum thiolates may also be used as a general predictor of the O_{oxo}−Mo−$S_{thiolate}$−C dihedral angle (x) according to

$$\frac{I_{xz,yz}}{2I_{xy}} = \frac{\cos^2 (90° - x) \times (14.7)}{\cos^2 (x) \times (25)} \qquad (2)$$

Using the experimental $I_{xz,yz}/2I_{xy}$ = 1.3 intensity ratio, application of eq 2 yields an O_{oxo}−Mo−$S_{thiolate}$−C dihedral

(29) Shadle, S. E.; Hedman, B.; Hodgson, K. O.; Solomon, E. I. *J. Am. Chem. Soc.* **1995**, *117*, 2259−2272.

Table 3. Sulfur K-Pre-Edge $S^v(3p)$ Character Per Thiolate Covalently Mixed in to Mo(*xy*) and Mo(*xz*,*yz*) Orbitals

compound	peak 1 energy(eV)	% of total t_{2g} area − peak 1	%S per thiolate in the Mo(*xy*) redox orbital	peak 2 energy (eV)	% of total t_{2g} area − peak 1	%S character in the Mo(*xz*,*yz*) orbital
$[PPh_4][MoO(SPh)_4]$	2470.8	29	6.6%	2472.2	71	10.8%
Tp*MoO(SPh)Cl	2470.5	38	8.5%	2471.4	62	10.3%
Tp*MoO(mba)	−	−	0.0%	2471.9	100	14.7%
Tp*MoO(bdt)	2470.5	18	n.a.	2471.8	82	n.a.

angle of ∼56° for $[MoO(SPh)_4]^{1-}$, which is in excellent agreement with the average crystallographically determined $O_{oxo}-Mo-S_{thiolate}-C$ dihedral angle of 59°. The $I_{xz,yz}/2I_{yz}$ ratio for Tp*MoO(SPh)Cl is 0.8. The $I_{xz,yz}/2I_{xy}$ ratio reveals 8.5% and 10.3% thiolate $S^v(3p)$ orbital character covalently mixed in to Mo(*xy*) and Mo(*xz*,*yz*) respectively. Since the structure of Tp*MoO(SPh)Cl has yet to be determined, eq 1 predicts that the $O_{oxo}-Mo-S_{thiolate}-C$ dihedral angle in Tp*MoO(SPh)Cl is ∼50°. The S K-pre-edge-derived $S^v(3p)$ character per thiolate covalently mixed in to Mo(*xy*) and Mo(*xz*,*yz*) for $[MoO(SPh)_4]^{1-}$, Tp*MoO(SPh)Cl, and Tp*MoO(mba) is presented in Table 3 for comparative purposes.

It is clear from Figure 2 that the Tp*MoO(mba) S K-pre-edge data are markedly different from that observed for the oxomolybdenum thiolate complexes Tp*MoO(SPh)Cl, and $[MoO(SPh)_4]^{1-}$, or the dithiolene complex Tp*MoO(bdt). Specifically, no pre-edge feature, assignable as a $S(1s)\rightarrow S^v(3p) + Mo(xy)$ transition, is observed at ∼2470.5 eV for Tp*MoO(mba). The explanation lies in the ∼95° $O_{oxo}-Mo-S_{thiolate}-C$ dihedral angle for this compound, which precludes any significant overlap between the S^v and Mo(*xy*) orbitals. Therefore, there is no $S^v(3p)$ covalency contribution to the Mo(*xy*) redox orbital and, according to Figure 4, the dominant $S^v(3p)\rightarrow Mo(xz,yz)$ charge donation results in the full ∼14.5% $S^v(3p)$ orbital character covalently mixed into Mo(*xz*). Finally, the S K-pre-edge spectrum of the oxomolybdenum *dithiolene* compound, Tp*MoO(bdt), reveals that the $I_{xz,yz}/2I_{xy}$ intensity ratio is between that observed for oxomolybdenum thiolates and Tp*MoO(mba). Although the $O_{oxo}-Mo-S_{dihtiolene}-C$ dihedral angles in Tp*MoO(bdt) are similar to those of Tp*MoO(mba), a $S(1s)\rightarrow S(3p) + Mo(xy)$ transition is observed due to the pseudo-σ bonding interaction between Mo(*xy*) and the dithiolene $S^{ip}(a')$ orbital (Figure 3),[2] underscoring the inherent differences between oxomolybdenum thiolate and dithiolene bonding.[2] A detailed analysis of S K-edge spectra for various Tp*MoO(dithiolene) complexes will be presented elsewhere.

Discussion

Sulfur K-pre-edge intensity ratios have been determined for the $S(1s)\rightarrow S^v(3p) + Mo(xy)$ and $S(1s)\rightarrow S^v(3p) + Mo(xz,yz)$ transitions in three oxomolybdenum thiolates, and the oxomolybdenum dithiolene compound Tp*MoO(bdt). The tetrathiolate, $[MoO(SPh)_4]^{1-}$, possesses a high degree of symmetry ($\sim C_4$), and the electronic structure of this compound has been extensively probed by low-temperature electronic absorption, magnetic circular dichroism, and resonance Raman spectroscopies.[12−14,27] Importantly, these spectroscopic probes have been used to evaluate and validate the results of detailed bonding calculations at the DFT level of theory. As such, the $[MoO(SPh)_4]^{1-}$ ion is arguably the most well-characterized oxomolybdenum thiolate system from an electronic structure point of view and was therefore chosen to calibrate S K-pre-edge intensity ratios, ($I_{xz,yz}/2I_{xy}$), to thiolate $S^v(3p)$ orbital character covalently mixed into the Mo(*xy*) and Mo(*xz*,*yz*) orbitals. The results of the analysis show that $S^v(3p)-Mo(xz,yz)$ and $S^v(3p)-Mo(xy)$ covalency is highly dependent on the $O_{oxo}-Mo-S_{thiolate}-C$ dihedral angle, resulting in highly anisotropic covalency contributions to the oxomolybdenum thiolate bonding scheme for dihedral angles approaching 0°/180° (dominant covalency contribution to Mo(*xy*)) and 90°(dominant covalency contribution to Mo(*xz*,*yz*)). The use of ligand K-edge spectroscopy to provide second coordination sphere metric parameters (i.e., the $O_{ax}-Mo-S_{thiolate}-C$ dihedral angle) in oxomolybdenum thiolates extends the power of XAS as a structural probe.

The compound Tp*MoO(mba) represents the first structurally characterized oxomolybdenum monothiolate to possess an ∼90° $O_{oxo}-Mo-S_{thiolate}-C$ dihedral angle, close to that found in the X-ray structure of chicken and plant SO[15,16] and similar to that observed in the bacterial SDH. The S K-pre-edge data clearly demonstrate that there is negligable S thiolate character covalently mixed into the Mo(*xy*) orbital of Tp*MoO(mba), a very unusual situation for oxomolybdenum thiolates. The lack of $Mo(xy)-S^v(3p)$ covalency in Tp*MoO(mba) is confirmed by the absence of the low-energy (∼16 000 cm^{-1}) $S^v(3p)\rightarrow Mo(xy)$ charge-transfer transition characteristic of oxomolybdenum thiolate electronic absorption and MCD spectra.[10−13,18,19,30−32] Consistent with this idea is the fact that, to our knowledge, Tp*MoO(mba) possesses the lowest g_{iso}/A_{iso}^{Mo} ratio of any oxomolybdenum thiolate complex. The value of g_{iso} is sensitive to the degree of thiolate ligand character covalently mixed into Mo(*xy*) and the presence of low-energy $S^v(3p)\rightarrow Mo(xy)$ charge-transfer transitions.[11,21,22,33,34] The ligand-field model allows for ligand-field excited states to be mixed into the ground state via the spin−orbit operator, and predicts $g_{iso} < g_e$ for d^1 Mo(V) complexes. Thiolate character covalently mixed into the Mo(*xy*) redox orbital opposes the ligand-field contribution and increases the value of g_{iso}. Furthermore, $S^v(3p)\rightarrow Mo(xy)$ charge-transfer states are often observed at energies comparable to, or less than, the lowest energy ligand

(30) Helton, M. E.; Pacheco, A.; McMaster, J.; Enemark, J. H.; Kirk, M. L. *J. Inorg. Biochem.* **2000**, *80*, 227−233.
(31) Carducci, M. D.; Brown, C.; Solomon, E. I.; Enemark, J. H. *J. Am. Chem. Soc.* **1994**, *116*, 11856−11868.
(32) McMaster, J.; Carducci, M.; Yang, Y.; Solomon, E.; Enemark, J. *J. Inorg. Biochem.* **1999**, *74*, 229.
(33) Nipales, N. S.; Westmoreland, T. D. *Inorg. Chem.* **1995**, *34*, 3374−3377.
(34) Nipales, N. S.; Westmoreland, T. D. *Inorg. Chem.* **1997**, *36*, 756−757.

field states.[2,10,12−14,27,31,35] Therefore, these low-energy S^{v}(3p)→Mo(*xy*) charge-transfer states can also efficiently mix with the ground state under the spin orbit operator.[11] This results in a further increase in g_{iso} since the charge-transfer contributions to the *g* value oppose ligand field contributions. This derives from the change in sign of the ligand-derived spin−orbit matrix elements relative to those of the metal.[21,34] Experimentally, this results in $g_{iso} \sim g_e$ for many oxomolybdenum thiolates. The isotropic metal hyperfine coupling constant, A_{iso}^{Mo}, is affected in a similar way and is reduced due to the presence of S^{v}(3p)−Mo(*xy*) covalency. As there is no S^{v}(3p) covalency contribution to Mo(*xy*) in Tp*MoO(mba) and this compound does not possess a low-energy S^{v}(3p)→Mo(*xy*) charge-transfer transition, the g_{iso}/A_{iso}^{Mo} ratio is low relative to other oxomolybdenum thiolates, including both *hpH* and *lpH* SO. Provided the O_{oxo}−Mo−$S_{thiolate}$−C dihedral angle in *hpH* and *lpH* SO is the same as in the X-ray structure of the chicken enzyme, S^{v}(3p)−Mo(*xy*) covalency is minimized and the larger enzyme g_{iso}/A_{iso}^{Mo} ratios likely result from dominant $S_{dithiolene}$(3p)−Mo(*xy*) and $S_{dithiolene}$(3p)−Mo(*xz*,*yz*) orbital interactions, as opposed to $S_{thiolate}$(3p)−Mo(*xy*) covalency.

Collectively, these results have intriguing implications regarding the electron-transfer half-reaction in SO. Low-energy charge-transfer transitions in the Mo(VI) absorption spectrum of the *A. thaliana* enzyme ,[9] which lacks the *b*-heme chromophore of vertebrate SO, and EPR simulations of the *lpH* and *hpH* forms of SO[36] suggest that there is considerable spin density delocalized onto the dithiolene and/or cysteine thiolate sulfur donor ligands in the Mo(V) form of the enzyme. The crystallographic O_{ax}−Mo−S_{Cys}−C dihedral angles determined for the chicken, plant, and bacterial enzymes are 80°, 74°, and 72°, respectively. However, the *hpH* EPR *g* values for these enzymes are essentially identical, indicating that the variability in crystallographic O_{ax}−Mo−S_{Cys}−C dihedral angles is not apparent in the Mo(V) form of the enzymes at high pH. Additionally, our calculations on a model for SO_{red} indicate that the most stable geometry is one with a O_{oxo}−Mo−S_{Cys}−C dihedral angle of 80°, essentially identical to that found in the chicken enzyme. Our results, coupled with the structural, EPR, and computational data on reduced forms of SO or SDH, allow for an approximate determination of the percentage of S_{Cys}^{v}(3p) character covalently mixed into the Mo(*xy*) orbital in reduced enzyme forms according to

$$\%\text{S character} = \cos^2(x) \times (25) \qquad (3)$$

Using an O_{oxo}−Mo−S_{Cys}−C dihedral angle of 80°, this results in a mere 0.75% S_{Cys}^{v}(3p) character covalently mixed into the Mo(*xy*) redox orbital, and this compares remarkably well with the ∼1% S_{Cys}^{v}(3p) character in the Mo(*xy*) orbital of a recent computational model for SO_{red}.[13] Interestingly, the recent structure of *S. novella* SDH reveals that the Mo center is only 8.5 Å from the heme propionate of its redox partner.[17] Here, electron transfer has been suggested to be mediated by a hydrogen-bonding network connecting the Mo-bound H_2O/OH^- to the heme propionate via Arg-55A or via a series of aromatic amino acid residues (Phe-168A, Tyr-236A, Trp-231A, Phe-230A, and Tyr-61B) where Phe-168A and Tyr-61B directly interact with the pyranopterin and heme cofactors, respectively. Thus, it appears unlikely that electron transfer out of the Mo active site is mediated by the coordinated cysteine thiolate in this geometry. However, electron-transfer regeneration could be mediated by the pyranopterin dithiolene in SO/SDH, and this would be consistent with previous studies that suggested the pyranopterin dithiolene could effectively couple the active site to hole superexchange pathways for electron-transfer regeneration via a pseudo-σ $S_{dithiolene}$(3p)−Mo(*xy*) interaction.[2,37]

Finally, the S K-pre-edge data presented here reveal the inherent electronic structure differences between dithiolene and thiolate donors. Namely, oxomolybdenum dithiolenes possess a higher degree of anisotropic Mo−S covalency when compared with typical oxomolybdenum thiolates that possess O_{oxo}−Mo−S_{Cys}−C dihedral angles of ∼60°, and this results from the unique oxomolybdenum-dithiolene bonding scheme. The S K-edge data for Tp*MoO(bdt) indicate that the intensity of the S(1s)→S(3p) + Mo(*xy*) transition in oxomolybdenum dithiolenes will serve as a direct probe of the important pseudo-σ $S_{dithiolene}$(3p)−Mo(*xy*) bonding interaction hypothesized to play a key role in facilitating electron-transfer regeneration in pyranopterin molybdenum enzymes.

Conclusions

The crystallographic and S K-edge XAS characterization of Tp*MoO(mba) has made it possible to show that O_{oxo}−Mo−$S_{thiolate}$−C dihedral angles near 90° severely attenuate thiolate covalency contributions to the Mo(*xy*) redox orbital. Expressions have been developed, based on the results of previous DFT calculations,[13] and evaluated by S K-edge XAS, which relate ligand K-edge intensity ratios to a second coordination sphere structural parameter, namely the O_{oxo}−Mo−$S_{thiolate}$−C dihedral angle, in oxomolybdenum thiolates. These results further increase our understanding of thiolate ligand contributions to reduction potentials, redox kinetics, and electron-transfer rates at oxomolybdenum thiolate sites. Additionally, this work provides a framework for understanding geometric/electronic structure relationships in *hpH*, *lpH*, and various mutant forms of SO, particularly with respect to how the O_{oxo}−Mo−$S_{thiolate}$−C dihedral affects the electronic structure and function of the molybdenum center. In summary, the remarkable agreement between theory and experiment presented here provides a basis for using S K-edge spectroscopy to determine the relationships between covalency and structural parameters in other oxo-metal

(35) Inscore, F. E.; McNaughton, R.; Westcott, B. L.; Helton, M. E.; Jones, R. M.; Dhawan, I. K.; Enemark, J. H.; Kirk, M. L. *Inorg. Chem.* **1999**, *38*, 1401−1410.
(36) Dhawan, I. K.; Enemark, J. H. *Inorg. Chem.* **1996**, *35*, 4873−4882.
(37) Enroth, C.; Eger, B.; Okamoto, K.; Nishino, T.; Nishino, T.; Pai, E. *Proc. Nat. Acad. Sci. U.S.A.* **2000**, *97*, 10723−10728.

thiolates and dithiolenes, and this represents ongoing work in our laboratories.

Acknowledgment. M.L.K. acknowledges the National Institutes of Health (GM-057378) for financial support of this work.

Supporting Information Available: Crystallographic data in CIF format. This material is available free of charge via the Internet at http://pubs.acs.org.

IC061150Z